An evaluation of geothermal energy potential in South Africa using geothermal fluid chemistry

Musarrat Safi.[1]*, Taufeeq Dhansay[1]*,
Council for Geoscience
Email: msafi@geoscience.org.za, tdhansay@geoscience.org.za

Acknowledgements

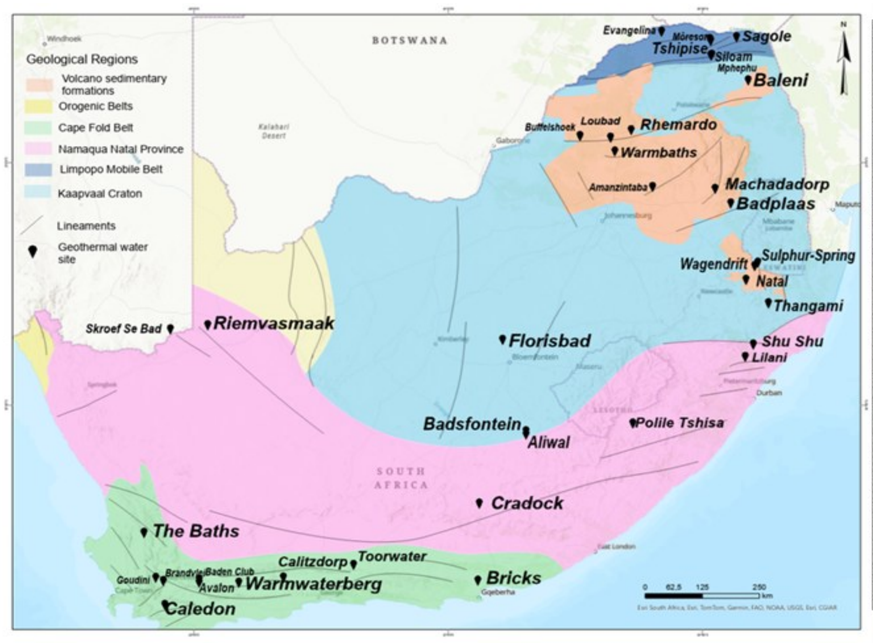
Special thanks to the privately owned, municipality owned, community owned geothermal waters, spas, hotels and game reserves for granting the Council for Geoscience team access to work in the area.

mineral & petroleum resources
Department: Mineral and Petroleum Resources
REPUBLIC OF SOUTH AFRICA

Council for Geoscience

ABSTRACT

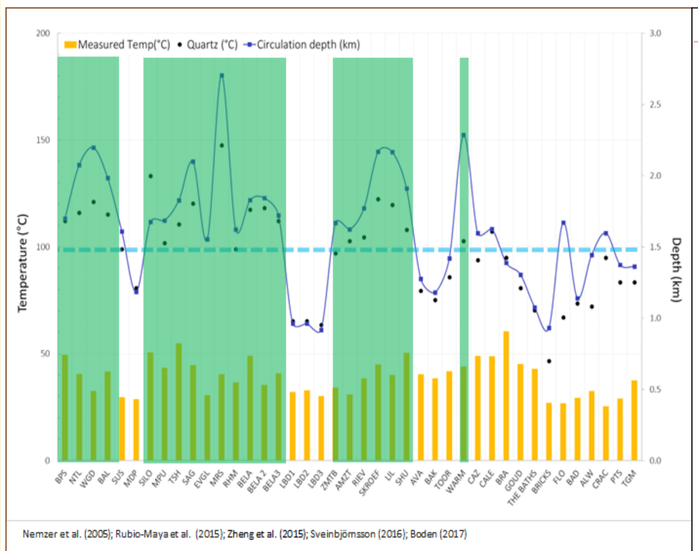
The literature on the **characteristics of geothermal water** sites in South Africa is limited. Additional information is required to identify potential sites for the utilisation of geothermal energy for power generation. Hence this study **presents the findings of new data collected from forty-one sites in South Africa.** (Fig. 1).



Geothermal water sites	Abbreviation
Badplaas	BPS
Natal	NTL
Wagendrift	WGD
Baleni	BAL
Sulphur Spring	SUS
Machadodorp	MDP
Siloam	SILO
Mphephu	MPU
Tshipise	TSH
Sagole	SAG
Evangelina	EVGL
Môreson	MRS
Rhemardo	RHM
Warmbath1	BELA
Warmbath2	BELA 2
Warmbath3	BELA3
Loubad1	LBD1
Loubad2	LBD2
Loubad3	LBD3
Amanzintaba	AMZT
Zimthabi	ZMTB
Riemvasmaak	RIEV
Skroef Se Bad	SKROEF
Lilani	LIL
Shu Shu	SHU
Avalon	AVA
Baden Club	BAK
Toorwater	TOOR
Warmwaterberg	WARM
Calitzdorp	CAZ
Caledon	CALE
Brandvlei	BRA
Goudini	GOUD
The Baths	THE BATHS
Bricks	BRICKS
Florisbad	FLO
Badsfontein	BAD
Aliwal	ALW
Cradock	CRAC
Polile Tshisa	PTS
Thangami	TGM

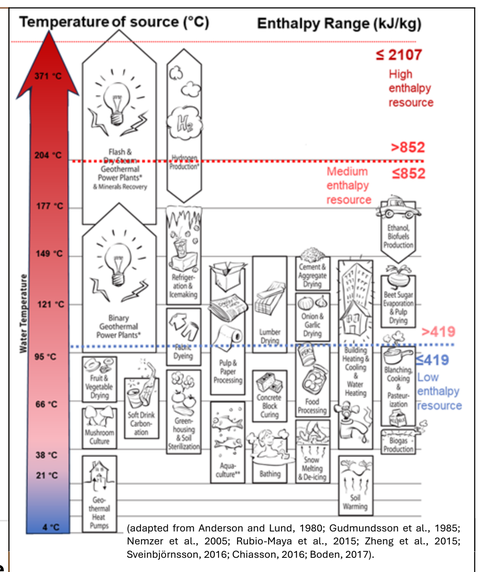
Figure 1. The location of the forty-one geothermal water sites sampled and associated geological regions (adapted from Dhansay et al, 2017) .

TAKE HOME MESSAGE: GEOTHERMAL ENERGY POTENTIAL IN SOUTH AFRICA



Nemzer et al. (2005); Rubio-Maya et al. (2015); Zheng et al. (2015); Sveinbjömsson (2016); Boden (2017)

Figure 2. Circulation depth (km), measured temperature of the geothermal waters at surface (°C) and quartz geothermometry temperatures (°C) (adapted from Dhansay et al. 2017).



(adapted from Anderson and Lund, 1980; Gudmundsson et al., 1985; Nemzer et al., 2005; Rubio-Maya et al., 2015; Zheng et al., 2015; Sveinbjörnsson, 2016; Chiasson, 2016; Boden, 2017).

Figure 3. Lindal diagram showing the utilisation of geothermal resource at temperatures and enthalpy ranges.

By utilising geothermal gradient and the geothermometry, the depth of the geothermal waters are between 1-3 km below surface (Fig. 2).

Nineteen sites across the country exhibit low to medium enthalpy Ranges (Fig. 3).

Future endeavours include feasibility studies.

MATERIALS AND METHOD

HYDROCHEMISTRY

Physical properties were measured with a **multi-sensor probe for temperature, pH and total electrical conductivity (EC).** The geothermal waters were sampled as established by Weaver et al., (2007) (Fig. 4). The analytical precision is estimated at 0.5‰ for δ18O and 1.5‰ δD, expressed relative to Local Meteoric Water Line (LMWL).

Analyses were completed utilising various instruments such as **induced coupled plasma-optical emission spectrometer, discrete analyzer, spectro-photometer and isotope ratio mass spectrometer.**

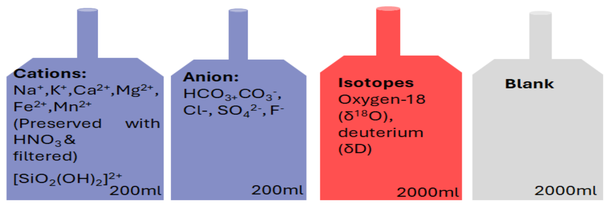


Figure 4. Hydrochemistry sampling showing the composition analysed and the volume (mL) of geothermal water collected per site.

CIRCULATION DEPTH OF GEOTHERMAL WATERS

Depths were calculated according to the equation

z=Tcalc-Tavg/ G

where z = the geothermal resource depth in meters, Tcalc = temperature (°C) calculated by a reliable geothermometer, T avg = yearly average air temperature (°C) of the sampling locality, G = mean geothermal gradient (Cave & Clark, 2003, Shestakova et al. 2018, Chimeddorj et al. 2021).

RESULTS AND DISCUSSION

HYDROCHEMISTRY CLASSIFICATION

Based on the Piper diagram most of the geothermal waters sampled are classified as Na-Cl, some as Na-HCO_3, Mg-HCO_3 and mixed type (Fig. 5). Na-Cl signature could have originated from marine and deep ancient groundwater environments where central up-flowing zones of liquid-dominated hydrothermal systems (Fournier,1982) are encountered. Na-HCO_3 type waters are typical of deep groundwaters influenced by ion exchange contributing to an affinity to seawater. The mixed type represents a variety of environments such as deep ancient groundwaters, deeper groundwater influenced by ion exchange and/or shallow fresh groundwaters (Ármannsson, 2012; Stober and Bucher, 2013). The Mg-HCO_3 type signature is indicative of geothermal waters that occur deeper underground (Mohamed et al, 2015).

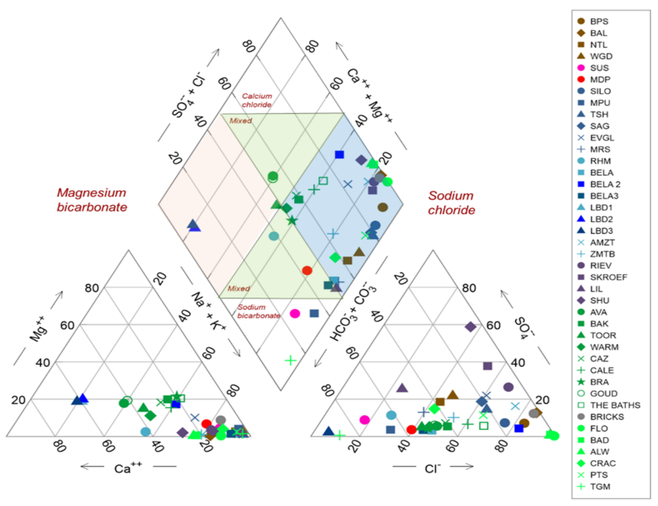


Figure 5. Piper diagram showing the geothermal waters are classified into four types of water (Piper, 1944; Bethke et al. 2022).

Fig. 6 isotopic data ranges from -13 ‰ to -39‰ δD and from −3.4 ‰ to -7.2 ‰ δ18O together with the Regional Meteoric Water Lines (MWL). **Enriched values** for δD have a closer affinity with sea waters. Furthermore, areas characterized by faults, which acted as conduits, may have resulted in connate waters influencing the source of geothermal waters. It is also possible that evaporation (Diamond and Harris, 2000) influenced the isotopic composition of geothermal waters. The **lighter isotope signatures** of plot below the Local Meteoric Line for most regions in South Africa indicative of longer residence time for the fractionation of the stable isotopes, but may also indicate that geothermal waters originate from deeper within the crust (Diamond and Harris, 2000; Mazor, 2003)

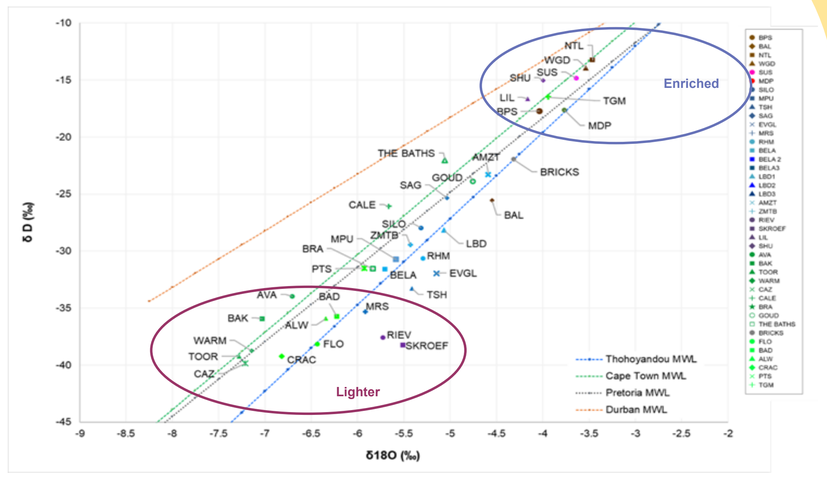


Figure 6. Isotopes compositions (δ18O versus δD) for the sampled geothermal waters together with Regional Meteoric Water Lines (MWL).

The **lighter isotope signatures** could have the same source that may have been affected by temperature (Geyh, 2000). Lastly, it is also possible that rainwater circulation through the source areas may have resulted in depleted isotopic signatures (Murray et al. 2015).

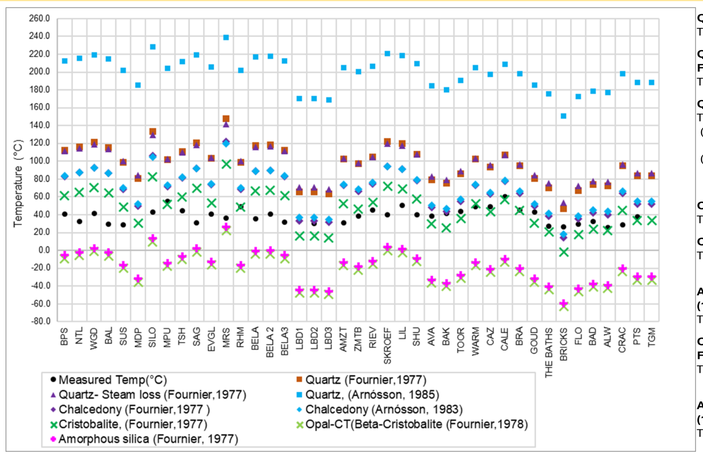


Figure 7. A comparison of calculated geothermometry (°C) utilising quartz concentrations.

Quartz- Fournier (1977)
$T_{SiO2} = \left(\frac{1309}{5.19 - \log Si}\right) - 273.15$

Quartz-after steam loss Fournier (1977)
$T_{SiO2} = \left(\frac{1522}{5.75 - \log Si}\right) - 273.15$

Quartz- Arnórsson (1985)
$T_{SiO2} = 53.50 + (0.011236Si) + (-0.5559x10^{-4}Si^2) + (0.1772 \times 10^{-7}\ Si^3) + (88.390 \log Si)$

Chalcedony- Fournier (1977)
$T_{SiO2} = \left(\frac{1032}{4.69 - \log Si}\right) - 273.15$

Chalcedony- Arnórsson (1983)
$T_{SiO2} = \left(\frac{1112}{4.91 - \log Si}\right) - 273.15$

Alpha-Cristobalite- Fournier (1977)
$T_{SiO2} = \left(\frac{1000}{4.78 - \log Si}\right) - 273.15$

Opal-CT(Beta-Cristobalite)- Fournier (1977)
$T_{SiO2} = \left(\frac{718}{4.51 - \log Si}\right) - 273.15$

Amorphous silica- Fournier (1977)
$T_{SiO2} = \left(\frac{731}{4.52 - \log Si}\right) - 273.15$

Fig. 7 represents the calculated reservoir temperature utilising quartz concentrations that range from -60 °C in BRICKS to 239 °C in Môreson (MRS). The opal-CT (Beta-Cristobalite), cristobalite and amorphous silica geothermometers are below 0°C .

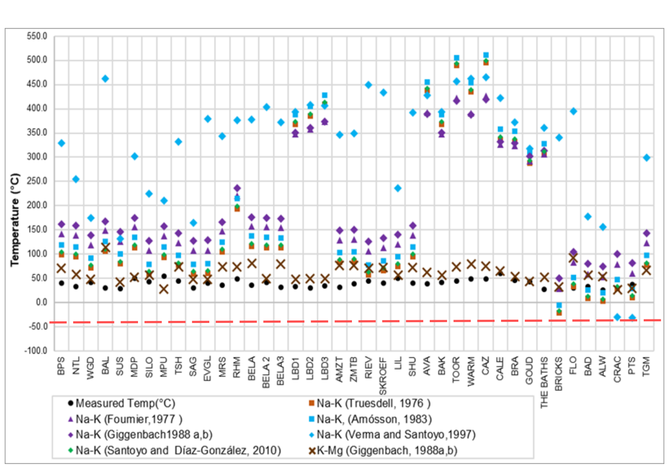


Figure 8. A comparison of calculated geothermometry (°C) utilising Na^+, K^+ and Mg^{2+} concentrations.

Na-K: Truesdell (1976)
$T_{Na/K} = \left(\frac{856}{\log\left(\frac{Na}{K}\right) + 0.857}\right) - 273.15$

Na-K: Fournier (1977)
$T_{Na/K} = \left(\frac{1217}{\log\left(\frac{Na}{K}\right) + 1.483}\right) - 273.15$

Na-K: Arnórsson (1983)
$T_{Na/K} = \left(\frac{933}{\log\left(\frac{Na}{K}\right) + 0.993}\right) - 273.15$

Na-K: Giggenbach (1988 a, b)
$T_{Na/K} = \left(\frac{1390}{1.750 + \log\left(\frac{Na}{K}\right)}\right) - 273.15$

Na-K: Verma and Santoyo (1997)
$T_{Na/K} = \left(\frac{1289}{\log\left(\frac{Na}{K}\right) + 1.615}\right) - 273.15$

Na-K: Santoyo and Díaz-González (2010)
$T_{Na/K} = \left(\frac{876.3(\pm 26.26)}{\log\left(\frac{Na}{K}\right) + 0.8775(\pm 0.0508)}\right) - 273.15$

K-Mg: Giggenbach (1988 a, b)
$T_{K/Mg} = \left(\frac{4410}{14 + \log\left(\frac{K^2}{Mg}\right)}\right) - 273.15$

Fig. 8 represents the calculated reservoir temperature utilising Na^+, K^+ and Mg^{2+} concentrations that range from -32°C at Polile Tshisa (PTS) to 511°C at Calitzdorp (CAZ).

REFERENCES

Arnórsson, S. Chemical equilibria in Icelandic geothermal systems-implications for chemical geothermometry investigations. Geothermics, **12**, (1983), 119-128.

Arnórsson, S. The use of mixing models and chemical geothermometers for estimating underground temperatures in geothermal systems. Journal of Volcanology and Geothermal Research, **23**, (1985), 299-335.

Bethke, C. M., Farrell, B. and Melika, S. The geochemist's workbench. Release 17. Aqueous Solutions, LLC, Champaign, Illinois (2022), 238pp.

Boden, D. R. Geologic fundamentals of Geothermal Energy. Taylor and Francis Group, CRC Press, Boca Raton, London, New York (2017), 381pp.

Boekstein, M. S. Hot spring holidays: Visitors' guide to hot springs and mineral spa resorts in southern Africa. Mark Boekstein, Cape Town (1998), 51pp.

Cave, L. and Clarke, S. A feasibility study on the use of chemical geothermometers for tracing deep groundwater flow. Water Research Commission report no. 1331/1/03. Water Research Commission. Pretoria, South Africa (2003), 53pp.

Chimeddorj, B., Munkhbat, D., Altanbaatar, B., Dolgorjav, O. and Oyuntsetseg, B. Hydrogeochemical characteristics and geothermometry of hot springs in the Altai region, Mongolia. Geochemistry: Exploration, Environment, Analysis, **21**, (2021), geochem2 021-016.

Dhansay, T. Shattered crust: how brittle deformation enables Critical Zone processes beneath southern Africa. South African Journal of Geology, **124(2)**, (2021), 519-536.

Dhansay, T., Musekiwa, C., Ntholi, T., Chevallier, L., Cole, D. and De Wit, M. J. South Africa's geothermal energy hotspots inferred from subsurface temperature and geology. South African Journal of Science, **113**, (2017), 1-7.

Fournier, R. O. Chemical geothermometers and mixing models for geothermal systems. Geothermics, **5**, (1977), 41–50.

Giggenbach, W. F. Graphical techniques for the evaluation of water/rock equilibration conditions by use of Na, K, Mg and Ca contents of discharge waters. Proceedings of the 8th New Zealand Geothermal Workshop, New Zealand (1986), 37-44.

Giggenbach, W. F. Geothermal solute equilibria. Derivation of Na–K–Mg–Ca geoindicators. Geochimica et cosmochimica acta, **52**, (1988 a, b), 2749-2765.

Henley, R. W., Truesdell, A.H., Barton, P. B. and Whitney, J. A. Fluid-mineral equilibria in hydrothermal systems. In: Reviews Economic Geology, Society of Economic Geologists, Yale (1984), 267pp.

Kent, L. E., 1949. The thermal waters of the union of South Africa and Southwest Africa. South African Journal of Geology, **52**, (1949), 231-264.

Nemzer, M., Page, D.S. and Carter, A.K. Energy for Keeps: Electricity from Renewable Energy: An Illustrated Guide for Everyone who Uses Electricity. Energy Education Group, California, USA (2005), 29-38.

Piper, A. M. A graphical procedure in the geochemical interpretation of water analyses. Eos Transactions American Geophysical Union, **25**, (1944), 914-923.

Santoyo, E. and Díaz-González, L. A new improved proposal of the Na/K geothermometer to estimate deep equilibrium temperatures and their uncertainties in geothermal systems. Proceedings World Geothermal Congress-2010. Bali, Indonesia (2010), 25-29.

Shestakova, A., Guseva, N., Kopylova, Y., Khvaschevskaya, A., Polya, D.A. and Tokarev, I. Geothermometry and isotope geochemistry of CO2-rich thermal waters in Choygan, East Tuva, Russia. Water, **10**, (2018), 729.

Sveinbjörnsson, B. M. Medium enthalpy geothermal systems in Iceland, thermal and electric potential. Iceland Geosurvey. Reykjavík, Iceland (2016). 123pp.

Tshibalo, A. E., Olivier, J. and Nyabeze, P. K. South Africa Geothermal Country Update (2010-2014). Proceedings of the World Geothermal Congress-2015, Melbourne, Australia (2015).

Truesdell, A. H. Summary of section III-geochemical techniques in exploration. Proceedings 2nd UN Symposium on the development and use of geothermal resources, 1, (1976), 1iii-1xxix.

Verma, S. P. and Santoyo, E. New improved equations for NaK, NaLi and SiO_2 geothermometers by outlier detection and rejection. Journal of Volcanology and Geothermal Research, **79**, (1997), 9-23.

Weaver, J. M. C., Cavé, L. and Talma, A. S. Groundwater Sampling: A comprehensive guide for sampling methods (2nd Edition). Water Research Commission report no. TT 303/07. Water Research Commission, Pretoria, South Africa (2007), 168pp.

Zheng, B., Xu, J., Ni, T. and Li, M. Geothermal energy utilization trends from a technological paradigm perspective. Renewable Energy, **77**, (2015), 430-441.